Chemical Engineering Journal 360 (2019) 542–552

Contents lists available at ScienceDirect

Chemical Engineering Journal

journal homepage: www.elsevier.com/locate/cej

In-situ construction of “octopus”-like nanostructure to achieve high performance epoxy thermosets

Zhengguang Heng, Xueqin Zhang, Yang Chen*, Huawei Zou*, Mei Liang

The State Key Lab of Polymer Materials Engineering, Polymer Research Institute of Sichuan University, Chengdu 610065, China

HIGHLIGHTS

- Octopus-like nanostructure was formed via incorporating block copolymer in epoxy.
- Nanostructure transformation during epoxy curing process were detailed investigated.
- Mechanical properties were significantly enhanced with low block copolymer content.
- Strengthening and toughening mechanisms of epoxy composites were thoroughly studied.

GRAPHICAL ABSTRACT

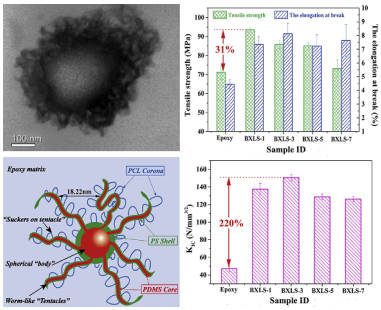

ARTICLE INFO

Keywords:
Block copolymer
Epoxy thermosets
High toughness
High strength
“Octopus”-like nanostructure

ABSTRACT

Inspired by the octopus, a typical nanostructure consisting of a spherical “body” and worm-like “tentacles with suckers” was constructed through incorporating polydimethylsiloxane-block-poly(ε-caprolactone)-block-polystyrene (BXLS) in epoxy thermosets. The novel nanostructure of BXLS copolymer and its morphology evolution during the epoxy curing process were investigated by transmission electron microscopy, field emission scanning electron microcopy and small-angle X-ray scattering. The mechanical properties of epoxy composites were significantly enhanced with a very low BXLS loading fraction. A 1.75 wt% of BXLS block copolymer could increase the tensile strength and fracture toughness up to 93.57 MPa and 137.43 N/mm$^{3/2}$, which were 1.31 times and 2.92 times that of the neat epoxy, respectively. Meanwhile, the toughening mechanism and the relationship between the high-performance properties of the epoxy composites and the nanostructure of the BXLS block copolymer were thoroughly studied. It is expected that our work can provide some new ideas and approaches for fabricating high-performance thermosets.

1. Introduction

Nature provides a wide range of materials with different structures that serve multiple related functions. These particular structures and functions have also inspired material scientists to solve a variety of technical challenges in materials science. The shock absorbing system [1] and superhydrophobic and ice-repellent material [2] were fabricated based on the woodpecker’s head and the microstructure on the surface of a lotus, respectively. It is well-known that epoxy is an important class of thermosets, however, its low fracture toughness greatly limits its application in high performance areas. Adding a second phase, such as thermoplastics [3–5], elastomers [6–8] and inorganic fillers [9,10] and their combination [11–13], is a technique commonly used to increase the fracture toughness of epoxy. However,

* Corresponding authors.
E-mail addresses: cy3262276@163.com (Y. Chen), hwzou@163.com (H. Zou).

https://doi.org/10.1016/j.cej.2018.12.020
Received 17 July 2018; Received in revised form 1 December 2018; Accepted 4 December 2018
Available online 05 December 2018
1385-8947/

many of these toughening agents are found inevitably to reduce other performances of epoxy composites such as the modulus and strength [11,14]. Thus, learning from nature and designing suitable microstructures have become the new tendencies in fabricating high-performance epoxy-based materials.

Over the past few decades, block copolymers endowed with epoxy-philic and epoxy-phobic blocks have emerged as efficient modifiers for improving the toughness of epoxy because they can self-assemble into a variety of nanostructures [15–20]. The toughening effectiveness of block copolymers is found to be dependent on the associated microphase separated nanostructures in the cured epoxy resins, including spherical micelles, vesicles, and wormlike micelles [18]. Dean et al. [21] reported that spherical micelles were found to improve the critical stress intensity factor (K_{IC}) by 25–35%, while a vesicular morphology was found to increase K_{IC} by 45% even at half the block copolymer concentration of the micelle forming system, which was further evidenced by the authors in another work [22]. Recent studies have shown that wormlike micelles have a more efficient toughening effect compared with the most common spherical nanodomains [23–25]. Study of Bates and co-workers [24] demonstrated that the critical stress intensity factor (K_{IC}) is 0.61 MPa*$m^{1/2}$ when spheres were constructed in DER383, whereas the K_{IC} of wormlike nanostructure modified epoxy was as high as 2.16 MPa*$m^{1/2}$. Nian et al. [26] studied the influence of nanostructures' morphologies on the fracture properties. The results indicated that branched wormlike micelles exhibited a higher degree of fracture toughness compared with the wormlike micelles modified epoxy system. Thus, it would be a promising way for fabricating high-performance thermosets through constructing worm-like derived nanostructures in the epoxy.

Inspired by the abovementioned studies, we aimed to explore the possibility of constructing special branched wormlike nanostructures that consist of a spherical "core-shell" body and worm-like "tentacles with suckers", similar to an octopus, via the suitable design of block copolymer. In this scenario, the advantages of both the spherical and branched worm-like nanostructures on toughening the epoxy could be maintained, meanwhile, the "suckers on tentacle" structure would further emphasize the interfacial bonding between the block copolymer phase and the epoxy matrix, thereby resulting in a greater improvement in toughness and tensile properties of epoxy composites. However, it is almost infeasible to construct such complex nanostructures in epoxy resin via a simple self-assembly [27,28] or reaction induced microphase separation [29–33] mechanism. Fortunately, the sequential phase separation method provided a possibility to achieve this goal [34–41]. For example, Fan et al reported that "core-shell" spherical micelles, wormlike and large-scaled lamellar nanostructures could be obtained by the "self-assembly-reaction induced microphase separation" (SA-RIMPS) method [34], meanwhile, cylinder and lamellar nanophases could be formed by "double reaction induced microphase separation" method [35]. Studies of Rebizant and coworkers [36,37] demonstrated that ordered raspberry-like nanostructures and wormlike micelles/vesicles were formed through the SA-RIMPS method in epoxy/polystyrene-polybutadiene-poly(methyl methacrylate) thermosets. In our previous work, we also utilized SA-RIMPS method to construct "soft core-rigid shell" nanostructures in epoxy/polystyrene-poly(ε-caprolactone)-polydimethylsiloxane-poly(ε-caprolactone)-polystyrene system [38]. Although the mechanisms of morphological transformation of block copolymer in the epoxy have been investigated in detail, studies on improving the mechanical properties of the epoxy by constructing nanostructures via the sequential phase separation of block copolymer, especially at low block copolymer loading, are rarely reported.

In the current work, a novel nanostructure that consists of a spherical "body" and worm-like "tentacles with suckers" is constructed in epoxy by designing polydimethylsiloxane-block-poly(ε-caprolactone)-block-polystyrene (BXLS) triblock copolymer via the SA-RIMPS sequential method. The morphology of the BXLS triblock copolymer and its transformation during the entire epoxy curing process are studied. To the best of our knowledge, this is the first report on this morphology nanostructure in epoxy. Meanwhile, the tensile properties and fracture toughness of the epoxy thermosets containing BXLS block copolymer are systematically investigated.

2. Experiment

2.1. Material

Epoxy precursor, diglycidyl ether of bisphenol A-based epoxy (Trade name: WSR-618), was obtained from Nantong Xingchen Synthetic Material Co., Ltd., China. Monohydroxyl-terminated polydimethylsiloxane (BX-OH, Trade name: X-22-107BX) was kindly supplied by the Shin-Etsu Chemical Co., Ltd., Japan. The monomer of ε-caprolactone (ε-CL), stannous octanoate [$Sn(Oct)_2$], N,N,N',N',N'-pentamethyldiethylenetriamine (PMDETA), 2-bromoisobutyryl bromide and copper(I) bromide (CuBr) were purchased from Aldrich Co., China. 4-Dimethylaminopyridine (DMAP) and 3,3′-dichloro-4,4′-diamino diphenyl methane (MOCA) were purchased from the Nanjing Tianhua Reagent Co., China and the Changshan beier Co., China, respectively. Styrene (St) and other solvents were purchased from the Chemical Reagent Factory of Kelong, China. Prior to processing, all of these materials were purified through the standard operations.

2.2. Synthesis of BXLS block copolymer

BXLS block copolymer was synthesized according to the literature [38,39] by the combination of the ring-opening polymerization (ROP) and atom transfer radical polymerization (ATRP). First, the BXL-OH block copolymer was synthesized via the ROP of ε-caprolactone (19.15 g, 167.98 mmol), which was initiated by monohydroxyl-terminated polydimethylsiloxane (BX-OH, 15 g, 3.83 mmol) with $Sn(Oct)_2$ (20 mg) as the catalyst. The above mixture was then immersed in a 120 °C oil bath for 48 h. Afterwards, the reaction between the BXL-OH block copolymer and 2-bromoisobutyryl bromide was performed to obtain the macroinitiator (BXL-Br). Finally, styrene monomers (9.47 g, 91.06 mmol), BXL-Br macroinitiator (17.2 g, 2 mmol), CuBr (340 mg), PMDETA (990 μL) and methylbenzene (solvent, 10 ml) were charged into a Schlenk flask to synthesize the BXLS block copolymer. The polymerization was conducted at 110 °C for 24 h. The crude product obtained in every step was allowed to drop into an excessive amount of cold methanol to afford the precipitates and then dried in a vacuum oven at 40 °C for 24 h to obtain the purified block copolymers.

2.3. Preparation of epoxy thermosets containing BXLS triblock copolymer

First, desired amounts of BXLS triblock copolymer and epoxy precursor were mixed with vigorous stirring at 130 °C. Then, the curing agent MOCA was added. Continuous stirring was performed until the mixtures became homogeneous. After being degassed in a 100 °C vacuum oven, the blends were poured into Teflon molds and subjected to thermal curing at 150 °C for 2 h and 180 °C for 2 h for post curing. The formulation of the nanostructured epoxy thermosets are presented in Table 1.

Table 1
The formulation of epoxy thermosets containing BXLS triblock copolymer.

Sample ID	EP (g)	MOCA (g)	BXLS (g)	BXLS (wt%)
EP	50	20	0	0
BXLS-1	50	20	1.25	1.75
BXLS -3	50	20	2.5	3.45
BXLS-5	50	20	3.75	5.08
BXLS-7	50	20	5	6.67
BXLS-22	50	20	20	22.22

3. Measurement and characterization

3.1. Nuclear magnetic resonance spectroscopy (NMR)

The obtained block copolymers were first dissolved in $CDCl_3$. Then, NMR measurements were conducted with a Bruker DRX-400 400 MHz NMR spectrometer (Germany) at room temperature.

3.2. Gel permeation chromatography (GPC)

The molecular weights of BX-OH and block copolymers were measured using a gel permeation chromatography (Waters 1515, USA), which is equipped with three columns (styragel @ HR THF, 7.8*300 mm) in series. The samples were analyzed at 30 °C with THF as the eluent, and the flow rate was set at 0.5 μL/min. Polystyrene (PS) was utilized as the calibration standards.

3.3. Transmission electron microscopy (TEM)

First, the epoxy thermosets containing BXLS block copolymers were cryogenically microtomed using an ultramicrotome (EM UC7, LEICA, Germany); the thickness of the ultrathin sections was 100–150 nm. The morphologies of the nanostructures were observed using a transmission electron microscope (TEM; Tecnai G2 F20, FEI, USA) with an acceleration voltage of 120 kV. Prior to observations, the ultrathin sections were stained with RuO_4 at room temperature for 20 min to enhance the electron density contrast.

3.4. Field emission scanning electron microcopy (FESEM)

The epoxy thermosets containing PCL-PDMS block copolymer were first fractured in liquid nitrogen and the fractured surface was coated with a thin layer of gold before observation. The microstructure was evaluated by a field emission scanning electron microscope (Nova NanoSEM 450, FEI, USA) instrument with an acceleration voltage of 5 kV.

3.5. Small-angle X-ray scattering (SAXS)

The SAXS measurements were taken on the Xeuss 2.0 SAXS/WAXS system (Xenocs, France). All experiments were conducted with the radiation of X-ray (wavelength λ = 1.54 Å) at a generator voltage of 50 kV and a generator current of 0.6 mA. The cured epoxy samples were measured at room temperature, while the uncured epoxy thermosets containing 6.67 wt% of the BXLS block copolymer were measured at 150 °C, which was above the upper critical solution temperature of PS and the epoxy. Two-dimensional diffraction patterns were recorded using a PILATUS 3R 300 K detector. The intensity profiles were output as the plot of the scattering intensity (I) versus scattering vector, q = (4π/λ.) sin (θ/2) (θ = scattering angle).

3.6. Dynamic mechanical analysis (DMA)

A dynamic mechanical experiment was conducted using a dynamic-mechanical thermal analyzer (Q800 DMA, TA Instruments, USA), with a three-point bending mode at 1 Hz. The dimensions of the employed specimens were 20 mm × 10 mm × 4 mm, and the temperature ranged from −135 °C to 200 °C at a heating rate of 3 °C/min.

3.7. Differential scanning calorimetry (DSC)

The thermal behaviors of the BXLS triblock copolymer and epoxy thermosets containing the BXLS triblock copolymer were investigated using a differential scanning calorimeter (TA Q200, USA). The BXLS triblock copolymer was scanned from −20 °C to 140 °C at a heating rate of 20 °C/min, while the epoxy composites were scanned from 30 °C to 210 °C with the same heating rate.

3.8. Mechanical properties

The mechanical properties of the epoxy thermosets containing the BXLS triblock copolymers specimens were determined using an Instron 5567 universal testing instrument (USA) at a speed of 2 mm/min. All mechanical values were taken from an average of five specimens. The fracture toughness was measured by the notched three-point bending test. The sample dimensions and testing procedures were summarized in ASTM standard D5045. The testing speed was 2 mm/min. The critical stress intensity factors (K_{IC}) were calculated using the following equation:

$$K_{IC} = \frac{SP}{BW^{\frac{3}{2}}} f(x)$$

$$f(x) = \frac{3\partial^{1/2}[1.99 - \partial(1-\partial)(2.15 - 3.93\partial + 2.7\partial^2)]}{2(1+2\partial)(1-\partial)^{3/2}}$$

$$\partial = \frac{A}{W}$$

where S was the testing span, P was the peak load, f was the shape factor, B was the specimen thickness, W was the specimen width and A was the crack length. The average K_{IC} was calculated as the arithmetic mean of five samples. The schematic diagram of the specimen is shown in Supplementary Fig. 1.

4. Results and discussion

4.1. Characterization of BXLS block copolymer

As mentioned above, the linear BXLS triblock copolymer was synthesized via a combination of the ring-opening polymerization (ROP) and atom transfer radical polymerization (ATRP). The detailed process is depicted in Fig. 1.

Shown in Fig. 2 and Supplementary Fig. 2 are the ^{1}H NMR and GPC results of BX, the BXL diblock copolymer and the BXLS triblock copolymer. Each GPC curve displayed a unimodal peak, and the molecular weight of BX, the BXL diblock copolymer and the BXLS triblock copolymer were measured to be M_n = 3915 g/mol with M_w/M_n = 1.06, M_n = 8449 g/mol with M_w/M_n = 1.24 and M_n = 14034 g/mol with M_w/M_n = 1.22, respectively. The ^{1}H NMR result of the BXL-Br diblock copolymer indicated that the structural units of PCL were characterized by the signals of resonance at 1.35–1.41 ppm [$OCOCH_2CH_2\underline{\mathbf{CH_2}}CH_2CH_2$], 1.60–1.68 ppm [$OCOCH_2\underline{\mathbf{CH_2}}CH_2\underline{\mathbf{CH_2}}CH_2$], 2.28–2.38 ppm [$OCO\underline{\mathbf{CH_2}}(CH_2)_4$] and 4.04–4.07 ppm [$OCO(CH_2)_4\underline{\mathbf{CH_2}}$], whereas the units of PDMS were at 0.07–0.09 ppm [$Si(\underline{\mathbf{CH_3}})_2O$], suggesting that the linear BXL diblock copolymer contained the structural features from both BX and PCL. According to the ratio of the integral intensity of the peaks at 2.28–2.38 ppm to that at 0.07–0.09 ppm, the molecular weight of the PCL subchain was calculated at 5472 g/mol, which had a good agreement with the result of GPC. With the inclusion of the PS subchain, new signals were detected at 6.3–7.2 ppm, which were attributed to [$CH_2CH\underline{\mathbf{C_6H_5}}$]. The detailed structure features of the BXLS triblock copolymer are marked in Fig. 2. Meanwhile, the molecular weight of the PS subchain was calculated to be 8008 g/mol depending on the ratio of integral intensity of the peaks at 6.3–7.2 ppm to that at 2.28–2.38 ppm. Therefore, it is reasonable to conclude that the linear BXLS triblock copolymer was successfully synthesized.

4.2. Morphology of the block copolymer in the epoxy matrix

Fig. 3 shows the TEM images of epoxy thermosets containing 1.75, 6.67 and 22.22 wt% of the BXLS triblock copolymer. The results showed that the BXLS triblock copolymer self-organized into microstructures

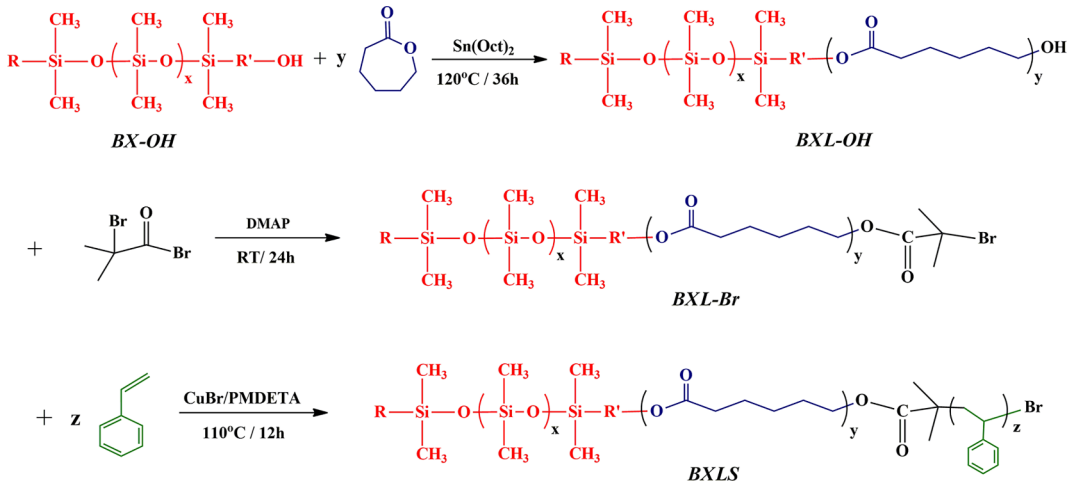

Fig. 1. Synthesis process of the BXLS block copolymer.

consisting of a spherical "body" and various "tentacles" after curing, which was contradictory to that reported by Fan et al. [34]. According to the dyeing mechanism, the darkest to the brightest domains in the TEM images should be the PS phase, the epoxy matrix, and then PDMS phase. Thus, the spherical "body" was attributed to the rich PDMS domain. When the content of the BXLS block copolymer was 1.75 wt% (Fig. 3a and a'), the diameter of the nanostructure and spherical rich PDMS domain were ~280 and ~120 nm, respectively. When further increasing the content of the BXLS block copolymer (Fig. 3b and b'), a morphology transformation of the microstructure was not observed. However, the diameters of the microstructure and spherical rich-PDMS domain increased to ~550 and ~250 nm, respectively.

To further clarify the detailed nanostructures, TEM images of epoxy containing 22.22 wt% of the BXLS block copolymer are displayed in Fig. 3c and c'. It is shown that the "tentacles" were connected to the surface of the spherical body and extended to the epoxy matrix. Meanwhile, the average distance between adjacent "tentacles" was measured to be ~18.22 nm. Both the spherical "body" and "tentacles" had a "core-shell" structure, where the PDMS segments constituted the soft core and the PS segments constituted the rigid shell. In light of the block sequence and the formation mechanisms of nanostructure [38], epoxy miscible PCL segments should be fixed surrounding the surfaces of the PS shell to form "coronas" after curing, which was similar to that of "tentacles with suckers". The specific diagram of this novel nanostructure is exhibited in Fig. 4. To the best of our knowledge, this typical nanostructure has never been reported before.

The SAXS results of the epoxy thermosets containing different concentrations of BXLS block copolymers are presented in Fig. 5. The SAXS curves of epoxy thermosets containing different contents of the BXLS block copolymers had a similar tendency, which means no morphology transformation occurred when increasing the concentration of the BXLS block copolymer. It was found that weak and broad shoulders were observed in the range of 0.005–0.02 $Å^{-1}$, which were attributed to the presence of a spherical "body". Although only broad shoulders were observed due to the amount and arrangement of the spherical "body", the shoulders became more and more obvious when increasing the content of the BXLS block copolymer. Meanwhile, a sharp peak at ~0.039 $Å^{-1}$ was present in each SAXS curve. According to the Bragg equation (L = 2π/Q), the average distance between neighboring phases was estimated to be 16.11 nm. Combined with the TEM observations, these scattering peaks should be ascribed to the "tentacle". The position of these peaks was almost unchanged when increasing the content of BXLS block copolymers, suggesting that the average distance between the neighboring "tentacle" was constant. The results of SAXS further

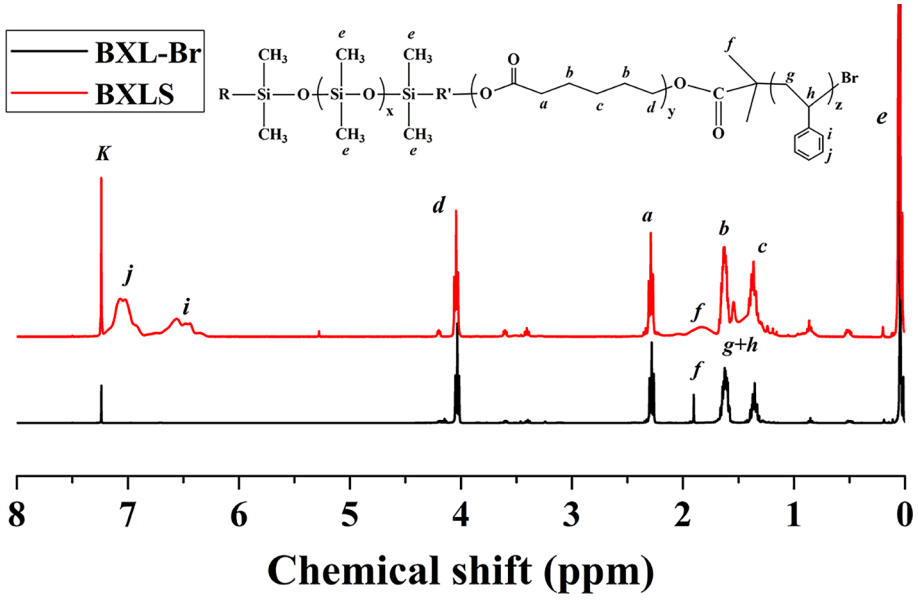

Fig. 2. ^{1}H NMR spectra of macroinitiator BXL-Br and the BXLS triblock copolymer.

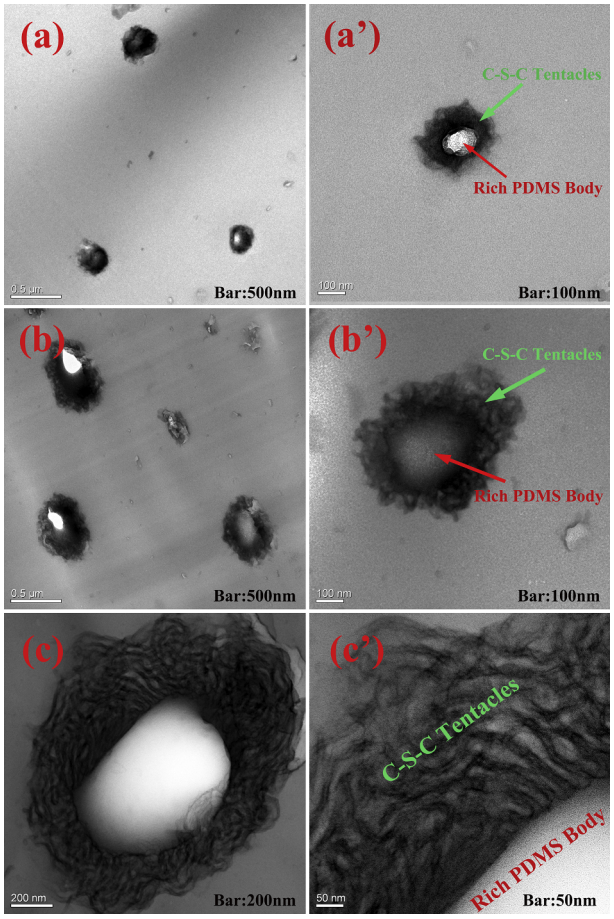

Fig. 3. TEM images of epoxy thermosets containing 1.75 (a and a'), 6.67 (b and b') and 22.22 wt% (c and c') of the BXLS block copolymer. [C-S-C, Core-Shell-Coronas].

confirmed the typical morphology observed in the TEM images.

4.3. Morphology evolution during the curing process

It has been reported that for a block copolymer constructed by PDMS, PCL and PS segments, the formation of nanostructures follows a two-step method, "self-assembly-reaction induced microphase separation" (SA-RIMPS) [34,38]. To investigate the formation of this special nanostructure, neat epoxy resin and epoxy thermosets containing

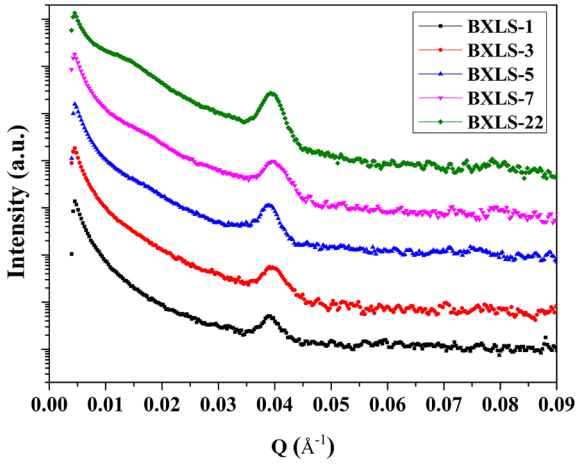

Fig. 5. SAXS spectra of epoxy thermosets containing 1.75, 3.45, 5.08, 6.67 and 22.22 wt% of BXLS block copolymer.

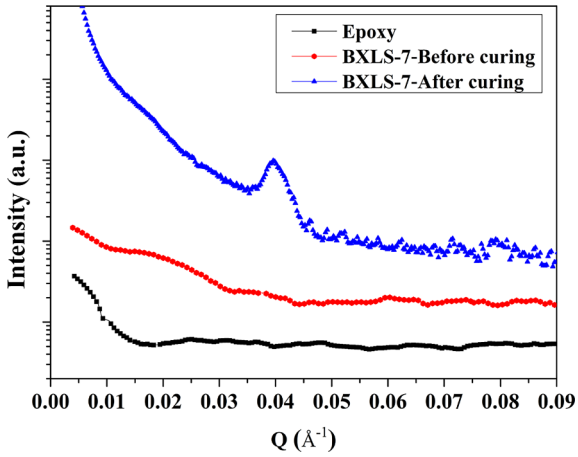

Fig. 6. SAXS spectra of epoxy and epoxy containing 6.67 wt% of the BXLS block copolymer before (150 °C) and after curing.

6.67 wt% BXLS block copolymer before and after curing were further measured by SAXS, as shown in Fig. 6. The testing temperature before curing was 150 °C, which was same as the first curing stage temperature and above the upper critical solution temperature of PS and epoxy. In this case, PDMS subchains were immiscible with epoxy, while both PCL and PS subchains were miscible with epoxy.

As for the neat epoxy, no scattering peaks or shoulders appeared in

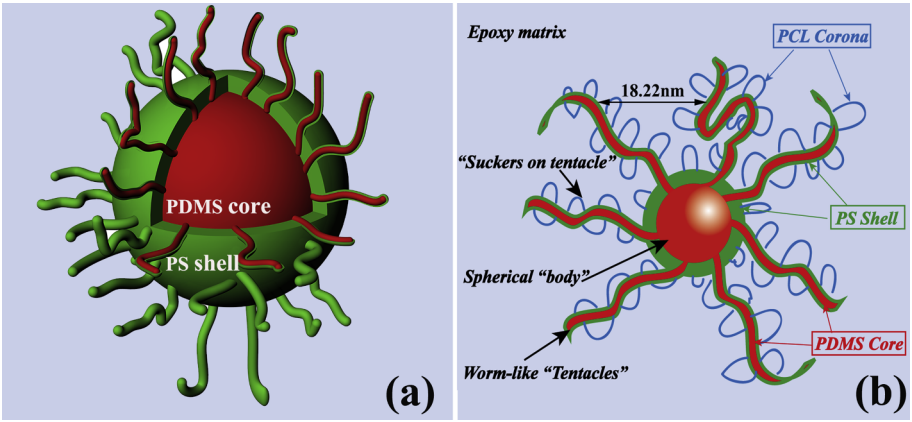

Fig. 4. Schematic diagram of the novel nanostructure. (a) 3D diagram, (b) Cross-sectional structure.

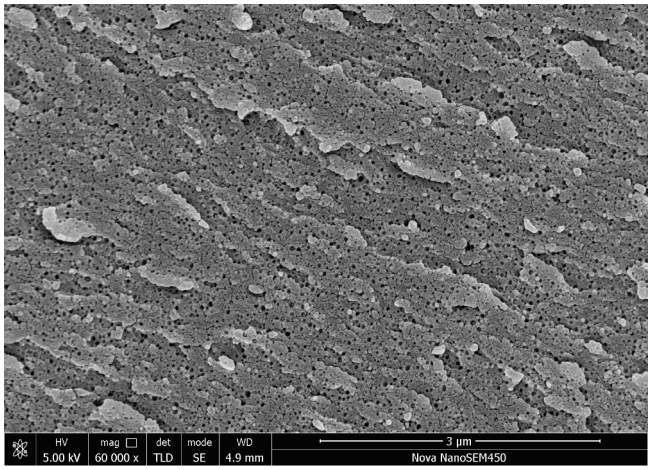

Fig. 7. FESEM image of epoxy containing 6.67 wt% of the BXL diblock copolymer.

the SAXS curve, indicating that no nanostructures were in the neat epoxy. When the BXLS block copolymer was incorporated, a scattering shoulder was observed before curing, which means the nanostructures already existed. In addition, the SAXS curve displayed a significant difference when the epoxy was completely cured, suggesting a morphology transformation occurred during the curing process and the final nanostructure was quite different with that prior to curing.

As for the self-assembly mechanism, block copolymers self-assembled into nanostructures before curing. Then, the formed nanostructures were fixed in the epoxy matrix and no morphology transformation occurred during the curing process [42]. Therefore, the nanostructure of the epoxy containing 6.67 wt% of the BXL block copolymer (the molecular weight of the BXL block copolymer was similar to that of the BXLS block copolymer and the length of miscible PCL subchain in the BXL was similar to the overall length of the PCL and PS subchains in the BXLS) was studied by FESEM, shown in Fig. 7. The results showed that BXL diblock copolymers self-assembled into spherical nanostructures. It is thus reasonable to speculate that BXLS block copolymers also self-assembled into spherical PDMS nanostructures before curing.

Therefore, the morphology transformation of the BXLS block copolymer during the curing process are illustrated in Fig. 8. First, PDMS blocks self-assembled into spherical nanostructures to form the spherical "body" prior to curing. Then, the reaction-induced microphase separation of the PS blocks occurred surrounding the PDMS nanostructures, leading to a decreased length of miscible blocks in the BXLS triblock copolymer. In this case, the interfacial curvature decreased, which made the formed nanostructures unstable, causing local recombination to occur during the curing process. Finally, novel nanostructures that consist of a spherical "body" and various "tentacles" were obtained. Meanwhile, PCL blocks would be still miscible with epoxy and fixed in the epoxy network to form "suckers", which can be corroborated by the results of DSC and DMA.

4.4. Compatible characterization of the BXLS block copolymer in epoxy thermosets

BXLS triblock copolymer and epoxy composites were measured via DSC to study the compatibility between the block copolymer and epoxy matrix, and the results were displayed in Fig. 9. Apart from the T_g of PS at 92 °C, the DSC curve of BXLS block copolymer also displayed a sharp endothermic peak at 49 °C, which was attributed to the PCL segments melting. However, the melting transformation of PCL was not observed in the DSC curves of epoxy composites, suggesting no PCL domains were formed and PCL subchains were still miscible with epoxy after curing. Meanwhile, it was determined that the T_gs of epoxy composites decreased with an increasing BXLS content, which had a good agreement with the results of DMA. Consistent with previous studies [43,44], the epoxy miscible PCL blocks acted as plasticizers, resulting in the glass transition temperature decreasing. Additionally, the plasticization effect was enhanced with an increase in the content of PCL. While the T_g of PDMS was not observed since it exceeded the lower limit of the testing temperature of TA Q200, the glass transitions of the rich-PDMS domains were observed in the DMA profile of the epoxy composites.

4.5. Dynamic mechanical analysis of epoxy containing BXLS block copolymer

The above nanostructured epoxy composites were also subjected to a dynamic mechanical analysis (DMA). The evolution of tan δ of epoxy thermosets containing the BXLS block copolymer versus temperature are shown in Fig. 10. For the neat epoxy, the glass transition temperature (T_g) was 179.1 °C. Apart from the α transition, two secondary transitions (viz. b-relaxation) at −64.4 °C and 77.8 °C were observed as well, which could be largely attributed to the motion of hydroxyl ether structural units and diphenyl groups in amine-crosslinked epoxy, respectively. When the BXLS block copolymer was incorporated, the curves exhibited a new glass transition at −129 °C, which can be ascribed to the motion of the rich-PDMS "body". Meanwhile, the transition peak became sharper and sharper with an increase in the content of the BXLS block copolymer. However, due to the plasticization of PCL, the T_gs of epoxy composites gradually decreased with an increase in the content of the BXLS triblock copolymer. The results of DMA and DSC further supported the novel morphology of nanostructures observed in Fig. 3.

Shown in Fig. 11 are the evolutions of the storage modulus and loss modulus of epoxy thermosets containing the BXLS block copolymer versus temperature. It is well-known that loss modulus is a measure of the energy dissipation. For epoxy thermosets containing 1.75, 5.08, 6.67 and 22.22 wt% of the BXLS block copolymer, the loss modulus was lower than that of neat epoxy when the temperature was under 130 °C. However, it is interesting to note that the capacity of energy dissipation for the epoxy thermosets containing 3.45 wt% of the BXLS block copolymer was higher than that of neat epoxy when the temperature was below 60 °C, suggesting that the energy dissipation capacity of epoxy thermosets containing 3.45 wt% of the BXLS block copolymer was better than that of the neat epoxy. As shown in Fig. 3, the diameters of the microstructure increased with an increase in the concentration of

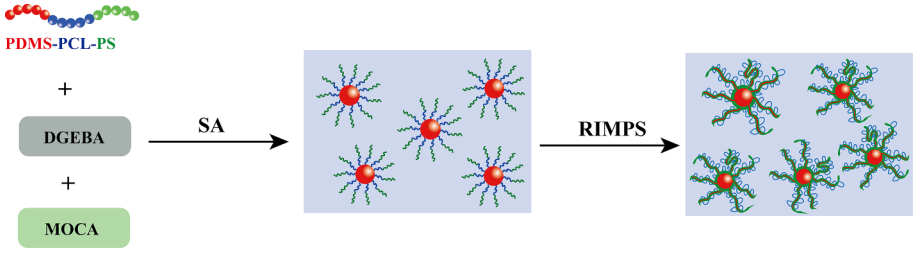

Fig. 8. Morphology transformation of the BXLS block copolymer during the curing process.

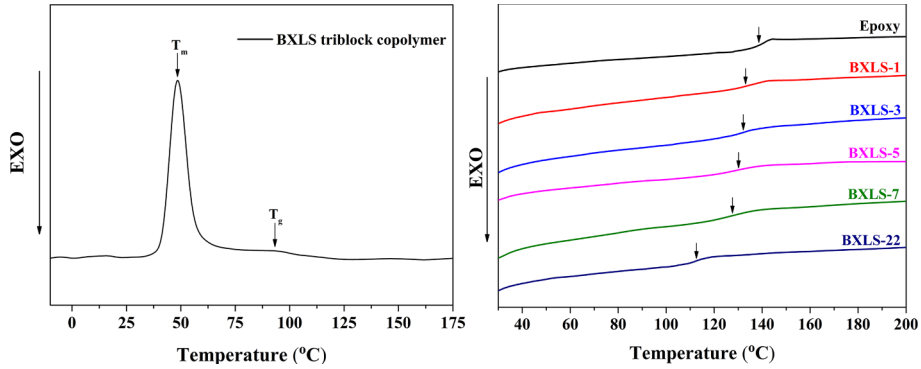

Fig. 9. DSC curves of the BXLS triblock copolymer and its epoxy composites.

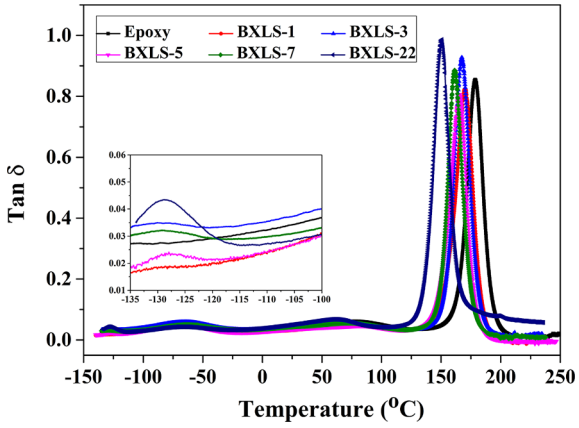

Fig. 10. Evolution of tan δ of epoxy thermosets containing BXLS block copolymer versus temperature.

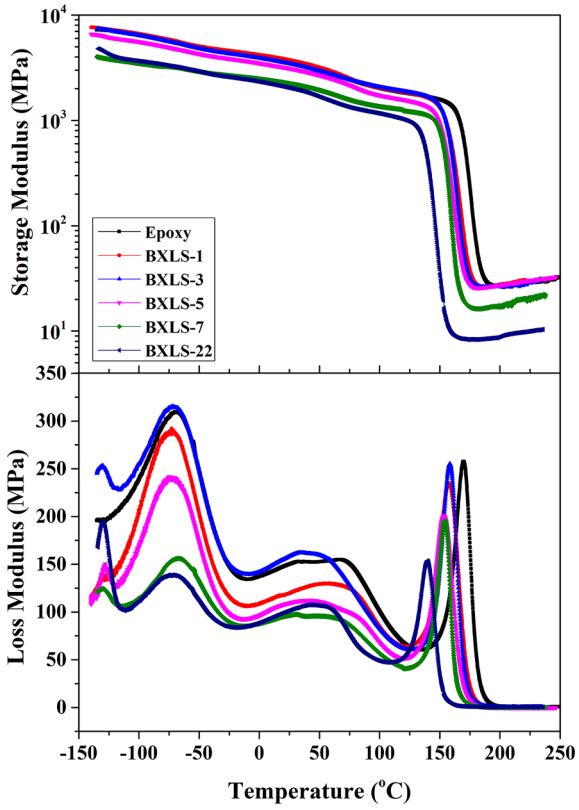

Fig. 11. Evolution of the storage modulus and loss modulus of epoxy thermosets containing BXLS block copolymer versus temperature.

the BXLS triblock copolymer. Thus, it can be deduced that the energy dissipation capacity of the epoxy composites had a close relationship with the size of the dispersed phase. Epoxy thermosets containing 3.45 wt% of BXLS block copolymer demonstrated the highest energy dissipation capacity, which could be further evidenced by the results of elongation at break and fracture toughness.

According to the theory of rubber elasticity, the cross-linking density (ν) of an epoxy network is proportional to its storage modulus in the rubbery region [45]. Thus, the cross-linking density was calculated using the following equation.

$$\nu = \frac{E'}{3RT}$$

where T is the absolute temperature of 20 °C above the glass transition temperature, E′ is the storage modulus at the corresponding temperature T and R is the gas constant. Corresponding values are listed in Table 2. It is shown that the cross-linking density slightly decreased when the content of the block copolymer was relatively low (1.75, 3.45 and 5.08 wt%). However, the cross-linking density of the epoxy thermosets was rapidly reduced when future increasing the content of the BXLS block copolymer, which could be caused by the gradual increase in the size of dispersed phases.

4.6. Mechanical properties of the epoxy thermosets containing the BXLS block copolymer

To verify the advantages of this novel nanostructure, epoxy thermosets containing different amounts of BXLS block copolymers were measured by a mechanical property test. The tensile properties of epoxy containing 0, 1.75, 3.45, 5.08 and 6.67 wt% of BXLS triblock copolymer are shown in Fig. 12. For the neat epoxy, the tensile strength and elongation at break were 71.3 MPa and 4.4%, respectively. It was found that tensile strength of all epoxy composites was improved by incorporating the BXLS block copolymer. The maximum tensile strength (93.6 MPa) was obtained for the epoxy thermosets containing 1.75 wt% BXLS, which was 1.31 times that of the neat epoxy. When further increasing the content of the BXLS block copolymer, the tensile strength gradually decreased; however, the values remained higher than that of

Table 2
DMA results of neat epoxy and epoxy thermosets containing the BXLS block copolymer.

Sample code	Storage modulus at 25 °C (MPa)	Tg (°C)	ν (mol/dm^3)
EP	3703	179.1	2.31
BXLS-1	3745	169.6	2.29
BXLS -3	3436	167.7	2.28
BXLS-5	3123	165.4	2.27
BXLS-7	2233	160.8	1.43
BXLS-22	2034	150.8	0.76

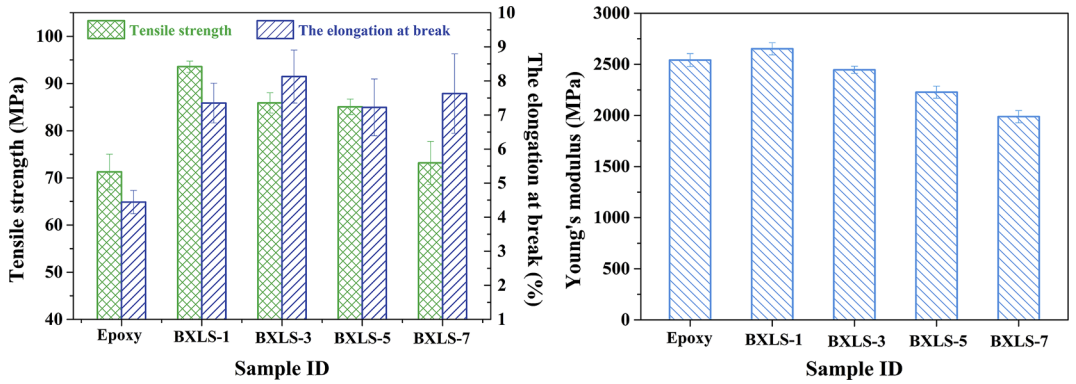

Fig. 12. Tensile properties of epoxy thermosets containing 0, 1.75, 3.45, 5.08 and 6.67 wt% of BXLS block copolymer.

the neat epoxy. The Young's modulus of the epoxy composites first increased then showed a decreasing trend as well when increasing the content of the block copolymer. However, only epoxy containing 1.75 wt% BXLS triblock copolymer was superior to neat epoxy.

This phenomenon could be explained by the nanostructure size, nanostructure morphology and crosslink density of the epoxy composites. Compared with the neat epoxy, the crosslink density of epoxy composites was almost unchanged, even for the BXLS-5 composites. TEM observations indicated that when the content of the BXLS block copolymer was at 1.75 wt%, the diameter of the spherical core–shell "body" was ~120 nm, which significantly increased the specific surface area of the separated domains and enhanced the interfacial bonding strength. Apart from the nanoscale spherical "body", the "tentacles" which were connected to the surface of the spherical "body" and extended to the epoxy matrix would make spherical "body" fixed in the epoxy matrix by physical interlocking and further increased the specific surface area of the BXLS block copolymer. It is known that the miscible PCL blocks form "coronas" after curing, and the appearance of "suckers" would further optimize the interactions between the BXLS block copolymer and matrix. Consequently, the interfacial adhesion between the nanostructure and epoxy matrix was greatly enhanced, thereby resulting in a higher tensile strength and Young's modulus. However, the diameter of the nanostructures increased with further increase in the content of the BXLS block copolymer, which lowered the specific surface area, leading to a reduction in the tensile strength and Young's modulus. Additionally, the decreased crosslink density would also reduce the tensile strength and Young's modulus. Because the crosslink density had a greater influence on the Young's modulus, only epoxy containing 1.75 wt% BXLS triblock copolymer was superior to neat epoxy.

The fracture toughness of the epoxy thermosets containing the BXLS block copolymer was evaluated by a three-point bending tests. The critical stress intensity factor (K_{IC}) was plotted as a function of the BXLS block copolymer content in Fig. 13. With increasing content of the BXLS block copolymer, the elongation at break and fracture toughness of the epoxy composites showed a similar trend. Both the elongation at break and the fracture toughness reached their maximum values at 3.45 wt% of the BXLS block copolymer, which were 1.84 times and 3.2 times that of the neat epoxy counterpart, respectively. When further increasing the content of the BXLS block copolymer, the elongation at break and fracture toughness slightly decreased before plateauing. It should be kept in mind that a significant improvement of fracture toughness can be achieved with the addition of merely 1.75 wt% BXLS block copolymer. For example, the K_{IC} of epoxy thermosets containing 1.75 wt% of BXLS block copolymer was 137.4 N/mm$^{3/2}$, which was 192% higher

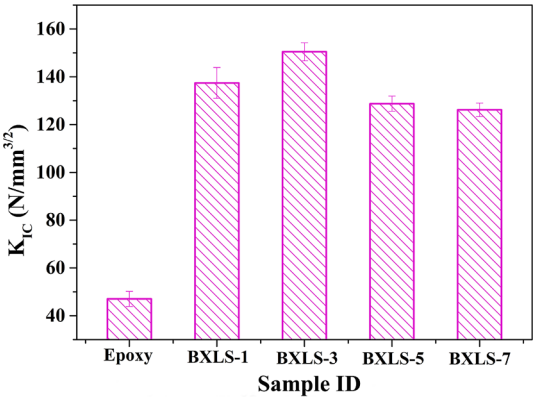

Fig. 13. Fracture toughness of epoxy thermosets containing 0, 1.75, 3.45, 5.08 and 6.67 wt% of the BXLS block copolymer.

than that of the neat epoxy. A comparison of the reported fracture toughness of epoxy composites as a function of modifier nanostructure and content is tabulated in Table 3. It is clear that our work outperformed others' in terms of the loading content of modifiers and enhancement of the fracture toughness.

The FESEM images of the fractured surface of neat epoxy and the epoxy thermosets containing 3.45 wt% BXLS block copolymer are given in Fig. 14. Fig. 14a–c shows that the fractured surface of the neat epoxy was very smooth at both low and high magnifications, indicating a brittle failure mode. However, the fractured surfaces of epoxy thermosets containing 3.45 wt% of the BXLS block copolymer were completely different compared with the neat epoxy. Due to the incorporation of the BXLS block copolymer, the fractured surface became rough and the roughness of the fractured surface gradually decreased along the white arrow, as shown in Fig. 14d. Moreover, the crack tips were likely to be blunted [52] due to the length to diameter ratio of connected "tentacles", which can be revealed by the high magnification FESEM images of the marked regions in Fig. 14d. These results indicated that crack deflection and blunting occurred when the crack propagated through the novel nanostructures. Furthermore, the spherical cavities and deformation of the nanostructures were also observed.

Normally, the worm-like structure facilitated the load transfer over a relatively large area, which enabled extensive plastic deformation and significantly enhanced the toughening effect [53]. A side-view of the crack tip region was characterized by the TEM, as displayed in Fig. 15. Bright rings with a diameter of 800–1000 nm were observed surrounding each dispersed phase, indicating that deformation of epoxy

Table 3
A comparison of the fracture toughness of epoxy thermosets as a function of the modifier structure and content.

Sample system	Content	Morphology	Improved Fracture Toughness	Ref.
GPG83/TDE85/DDS	2.5 wt%	Homogeneous	0.54 times	[46]
CSR-L/Epon828/DCD	22 vol%	Spherical	1.26 times	[7]
BCP/CSP/Epon862/DDS	3 phr/5 phr	Spherical	0.91 times	[47]
PCL_{62}-PI_{103}/EP/MOCA	20 wt%	Spherical	1.75 times	[48]
Silica/LR/DGEBA/MTHPA	12/9 vol%	Spherical	1.89 times	[49]
LSL/TGPAP/DDS	20 wt%	Spherical	0.23 times	[50]
CET61/DER332/THPE/BPA	5 wt%	Spherical	2.24 times	[51]
eSBS46-AEP/EP/DDM	5 wt%	Wormlike	0.54 times	[26]
EB3/Epon828/DMP30/C541	5 wt%	Wormlike/Spherical	1.45 times	[18]
EB2/Epon828/DMP30/C541	5 wt%	Branched wormlike	1.97 times	[18]
BXLS/DGEBA/MOCA	**1.75 wt%**	**“tentacle”-like nanostructures**	**1.92 times**	**Our work**
	3.45 wt%		**2.2 times**	

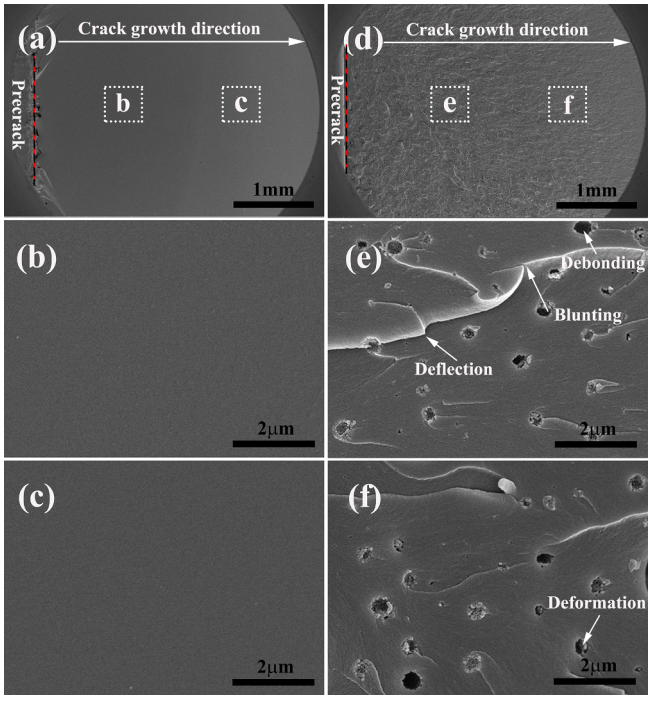

Fig. 14. FESEM images of the fractured surface of the neat epoxy (a, b, c) and epoxy thermosets containing 3.45 wt% BXLS block copolymer (d, e, f).

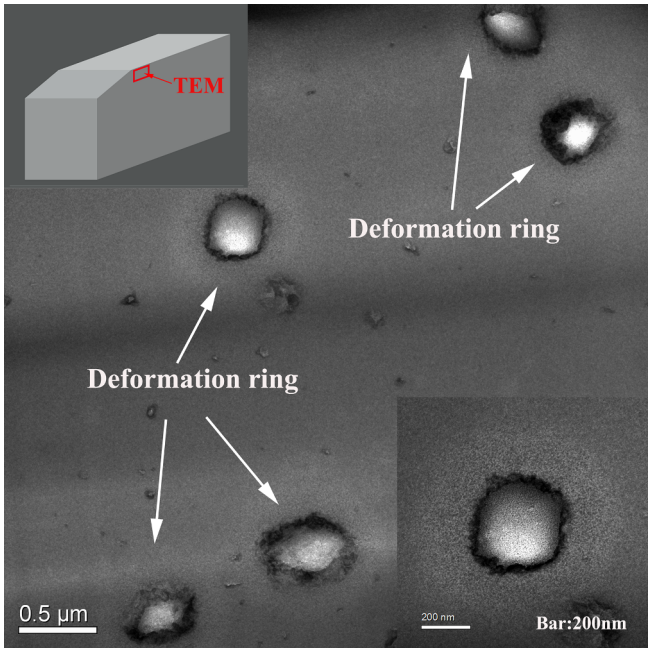

Fig. 15. TEM image of the side-view of crack tip region.

matrix occurred.

Therefore, it can be concluded that the improvement in toughness was derived from a combination of several toughening mechanisms: voiding or debonding, crack tip blunting and deflection, cavitation and deformation. The toughness mechanism of the novel nanostructure is shown in Fig. 16.

It is reported that the toughening effectiveness had a particle size dependence [5,11,14,44,54,55]. The TEM results showed that the diameter of the dispersed phase increased with an increased the content of the BXLS block copolymer. In addition, the results of the DMA indicated the epoxy thermosets containing 3.45 wt% of the BXLS block copolymer had the highest energy dissipation capacity. Thus, the maximum elongation at break and the fracture toughness of the epoxy composites were obtained when the content of BXLS was 3.45 wt%.

5. Conclusion

The fabrication of high-performance materials through the design of microstructures has become a new and popular trend. Inspired by nature, a novel nanostructure morphology that consists of a spherical “body” connected with wormlike “tentacles” was first constructed by incorporating polydimethylsiloxane-block-poly(ε-caprolactone)-block-polystyrene (BXLS) in epoxy thermosets. The morphology of this typical nanostructure was investigated using TEM and SAXS, and the morphology evolution during the epoxy curing process was studied using FESEM and SAXS. The mechanical properties of epoxy composites were obviously enhanced because of the presence of this typical “octopus”-like nanostructure. The tensile strength of the epoxy composites reached 93.57 MPa with the addition of only 1.75 wt% BXLS block copolymer, which was 1.31 times that of the neat epoxy. In addition, the elongation at break and fracture toughness were 1.84 times and 3.2 times that of the neat epoxy when the content of the block copolymer

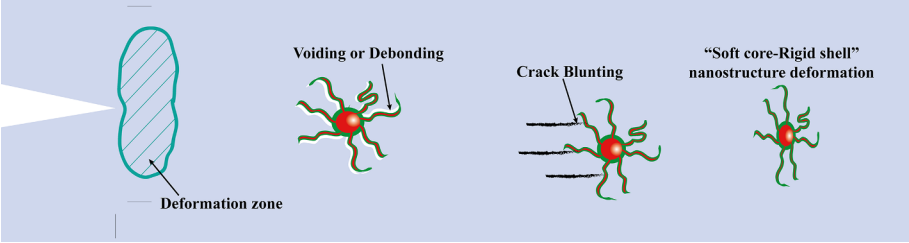

Fig. 16. Schematic diagram of toughness mechanism.

was 3.45 wt%, respectively. It is demonstrated that the remarkable enhancement in toughness was attributed to a combination of several toughening mechanisms: voiding or debonding, crack tip blunting and deflection, cavitation and deformation.

Acknowledgments

The authors thank the National Natural Science Foundation of China (51703137), the Fundamental Research Funds for the Central Universities (2012017yjsy186) and the Fundamental Research Funds for the Central Universities of China (2015SCU11008) for financial support. We would like to thank the Analytical & Testing Center of Sichuan University for transmission electron microscopy work and we would be grateful to Guiping Yuan for her help of TEM image.

Appendix A. Supplementary data

Supplementary data to this article can be found online at https://doi.org/10.1016/j.cej.2018.12.020.

References

[1] S.-H. Yoon, S. Park, A mechanical analysis of woodpecker drumming and its application to shock-absorbing systems, Bioinspir. Biomim. 6 (2011) 016003, , https://doi.org/10.1088/1748-3182/6/1/016003.
[2] L. Wang, Q. Gong, S. Zhan, L. Jiang, Y. Zheng, Robust anti-icing performance of a flexible superhydrophobic surface, Adv. Mater. 28 (2016) 7729–7735, https://doi.org/10.1002/adma.201602480.
[3] H. Shin, B. Kim, J.-G. Han, M.Y. Lee, J.K. Park, M. Cho, Fracture toughness enhancement of thermoplastic/epoxy blends by the plastic yield of toughening agents: a multiscale analysis, Compos. Sci. Technol. 145 (2017) 173–180, https://doi.org/10.1016/j.compscitech.2017.03.028.
[4] A.R. Jones, C.A. Watkins, S.R. White, N.R. Sottos, Self-healing thermoplastic-toughened epoxy, Polymer 74 (2015) 254–261, https://doi.org/10.1016/j.polymer.2015.07.028.
[5] B.B. Johnsen, A.J. Kinloch, A.C. Taylor, Toughness of syndiotactic polystyrene/epoxy polymer blends: microstructure and toughening mechanisms, Polymer 46 (2005) 7352–7369, https://doi.org/10.1016/j.polymer.2005.05.151.
[6] A.J. Kinloch, S.J. Shaw, D.A. Tod, D.H. Polymer, Deformation and Fracture Behaviour of a Rubber-toughened Epoxy: 1. Microstructure and Fracture Studies, Elsevier, (n.d.), 1983.
[7] D. Quan, A. Ivankovic, Effect of core–shell rubber (CSR) nano-particles on mechanical properties and fracture toughness of an epoxy polymer, Polymer 66 (2015) 16–28.
[8] J. Ma, M.S. Mo, X.S. Du, S.R. Dai, I. Luck, Study of epoxy toughened by in situ formed rubber nanoparticles, J. Appl. Polym. Sci. 110 (2008) 304–312, https://doi.org/10.1002/app.27882.
[9] T. Adachi, M. Osaki, W. Araki, S.-C. Kwon, Fracture toughness of nano- and micro-spherical silica-particle-filled epoxy composites, Acta Mater. 56 (2008) 2101–2109, https://doi.org/10.1016/j.actamat.2008.01.002.
[10] T.H. Hsieh, A.J. Kinloch, K. Masania, A.C. Taylor, S. Sprenger, The mechanisms and mechanics of the toughening of epoxy polymers modified with silica nanoparticles, Polymer 51 (2010) 6284–6294, https://doi.org/10.1016/j.polymer.2010.10.048.
[11] P.P. Vijayan, D. Puglia, M.A.S.A. Al-Maadeed, J.M. Kenny, S. Thomas, Elastomer/thermoplastic modified epoxy nanocomposites: the hybrid effect of 'micro' and 'nano' scale, Mater. Sci. Eng.: R: Reports 116 (2017) 1–29, https://doi.org/10.1016/j.mser.2017.03.001.
[12] K. Singh, T. Nanda, R. Mehta, Addition of nanoclay and compatibilized EPDM rubber for improved impact strength of epoxy glass fiber composites, Composites A 103 (2017) 263–271, https://doi.org/10.1016/j.compositesa.2017.10.009.
[13] S. Sprenger, Epoxy resins modified with elastomers and surface-modified silica nanoparticles, Polymer 54 (2013) 4790–4797, https://doi.org/10.1016/j.polymer.2013.06.011.
[14] M.L. Arias, P.M. Frontini, R.J.J. Williams, Analysis of the damage zone around the crack tip for two rubber-modified epoxy matrices exhibiting different toughenability, Polymer 44 (2003) 1537–1546, https://doi.org/10.1016/S0032-3861(02)00829-7.
[15] W.-C. Chu, W.-S. Lin, S.-W. Kuo, Flexible epoxy resin formed upon blending with a triblock copolymer through reaction-induced microphase separation, Materials 9 (2016) 449, https://doi.org/10.3390/ma9060449.
[16] A. Klingler, B. Wetzel, Fatigue crack propagation in triblock copolymer toughened epoxy nanocomposites, Polym. Eng. Sci. 57 (2017) 579–587, https://doi.org/10.1002/pen.24558.
[17] J. Chen, A.C. Taylor, Epoxy modified with triblock copolymers: morphology, mechanical properties and fracture mechanisms, J. Mater. Sci. 47 (2012) 4546–4560, https://doi.org/10.1007/s10853-012-6313-6.
[18] T. Li, M.J. Heinzer, L.F. Francis, F.S. Bates, Engineering superior toughness in commercially viable block copolymer modified epoxy resin, J. Polym. Sci., Part B: Polym. Phys. 54 (2016) 189–204, https://doi.org/10.1002/polb.23894.
[19] E. Serrano, A. Tercjak, C. Ocando, M. Larrañaga, M.D. Parellada, S. Corona-Galván, et al., Curing behavior and final properties of nanostructured thermosetting systems modified with epoxidized styrene-butadiene linear diblock copolymers, Macromol. Chem. Phys. 208 (2007) 2281–2292, https://doi.org/10.1002/macp.200700169.
[20] H. Kishi, Y. Kunimitsu, J. Imade, S. Oshita, Y. Morishita, M. Asada, Nano-phase structures and mechanical properties of epoxy/acryl triblock copolymer alloys, Polymer 52 (2011) 760–768, https://doi.org/10.1016/j.polymer.2010.12.025.
[21] J.M. Dean, P.M. Lipic, R.B. Grubbs, R.F. Cook, F.S. Bates, Micellar structure and mechanical properties of block copolymer-modified epoxies, J. Polym. Sci., Part B: Polym. Phys. 39 (2001) 2996–3010, https://doi.org/10.1002/polb.10062.
[22] J.M. Dean, R.B. Grubbs, W. Saad, R.F. Cook, F.S. Bates, Mechanical properties of block copolymer vesicle and micelle modified epoxies, J. Polym. Sci., Part B: Polym. Phys. 41 (2003) 2444–2456, https://doi.org/10.1002/polb.10595.
[23] J.M. Dean, N.E. Verghese, H.Q. Pham, F.S. Bates, Nanostructure toughened epoxy resins, Macromolecules 36 (2003) 9267–9270, https://doi.org/10.1021/ma034807y.
[24] Y.S. Thio, J. Wu, F.S. Bates, Epoxy toughening using low molecular weight poly (hexylene oxide) – poly(ethylene oxide) diblock copolymers, Macromolecules 39 (2006) 7187–7189, https://doi.org/10.1021/ma052731v.
[25] J. Wu, Y.S. Thio, F.S. Bates, Structure and properties of PBO-PEO diblock copolymer modified epoxy, J. Polym. Sci., Part B: Polym. Phys. 43 (2005) 1950–1965, https://doi.org/10.1002/polb.20488.
[26] F. Nian, J. Ou, Q. Yong, Y. Zhao, H. Pang, B. Liao, Reactive block copolymers for the toughening of epoxies: effect of nanostructured morphology and reactivity, J. Macromol. Sci., Part A 55 (2018) 533–543, https://doi.org/10.1080/10601325.2018.1476826.
[27] Paul M. Lipic, A. Frank, S. Bates, M.A. Hillmyer, Nanostructured thermosets from self-assembled amphiphilic block copolymer/epoxy resin mixtures, Am. Chem. Soc. (1998), https://doi.org/10.1021/ja981544s.
[28] S. Maiez-Tribut, J.P. Pascault, E.R. Soulé, A.J. Borrajo, R.J.J. Williams, Nanostructured epoxies based on the self-assembly of block copolymers: a new miscible block that can be tailored to different epoxy formulations, Macromolecules 40 (2007) 1268–1273, https://doi.org/10.1021/ma062185l.
[29] F. Meng, S. Zheng, W. Zhang, H. Li, Q. Liang, Nanostructured thermosetting blends of epoxy resin and amphiphilic poly(ε-caprolactone)-block-polybutadiene-block-poly(ε-caprolactone) triblock copolymer, Macromolecules 39 (2006) 711–719, https://doi.org/10.1021/ma0518499.
[30] E. Serrano, A. Tercjak, G. Kortaberria, J.A. Pomposo, D. Mecerreyes, N.E. Zafeiropoulos, et al., Nanostructured thermosetting systems by modification with epoxidized styrene – butadiene star block copolymers. Effect of epoxidation degree, Macromolecules 39 (2006) 2254–2261, https://doi.org/10.1021/ma0515477.
[31] Fanliang Meng, Sixun Zheng, Huiqin Li, A. Qi Liang, T. Liu, Formation of ordered nanostructures in epoxy thermosets: a mechanism of reaction-induced microphase separation, Macromolecules (2006), https://doi.org/10.1021/ma060004.
[32] Z. Xu, S. Zheng, Reaction-induced microphase separation in epoxy thermosets containing poly(ε-caprolactone)-block-poly(n-butyl acrylate) diblock copolymer, Macromolecules 40 (2007) 2548–2558, https://doi.org/10.1021/ma062486v.
[33] W. Fan, S. Zheng, Reaction-induced microphase separation in thermosetting blends of epoxy resin with poly(methyl methacrylate)-block-polystyrene block copolymers: effect of topologies of block copolymers on morphological structures, Polymer 49 (2008) 3157–3167, https://doi.org/10.1016/j.polymer.2008.05.010.

[34] W. Fan, L. Wang, S. Zheng, Nanostructures in thermosetting blends of epoxy resin with polydimethylsiloxane-block-poly(ε-caprolactone)-block-polystyrene ABC triblock copolymer, Macromolecules 42 (2008) 327–336, https://doi.org/10.1021/ma8018014.
[35] W. Fan, L. Wang, S. Zheng, Double reaction-induced microphase separation in epoxy resin containing polystyrene-block-poly(ε-caprolactone)-block-poly(n-butyl acrylate) ABC triblock copolymer, Macromolecules 43 (2010) 10600–10611, https://doi.org/10.1021/ma101945f.
[36] V. Rebizant, V. Abetz, F. Tournilhac, F. Court, L. Leibler, Reactive tetrablock copolymers containing glycidyl methacrylate. Synthesis and morphology control in epoxy–amine networks, Macromolecules 36 (2003) 9889–9896, https://doi.org/10.1021/ma0347565.
[37] V. Rebizant, A.-S. Venet, F. Tournilhac, E. Girard-Reydet, C. Navarro, J.-P. Pascault, et al., Chemistry and mechanical properties of epoxy-based thermosets reinforced by reactive and nonreactive SBMX block copolymers, Macromolecules 37 (2004) 8017–8027, https://doi.org/10.1021/ma0490754.
[38] Z. Heng, H. Zhang, Y. Chen, H. Zou, M. Liang, Controllable design of nanostructure in block copolymer reinforced epoxy composites, J. Appl. Polym. Sci. 135 (2018) 46362, https://doi.org/10.1002/app.46362.
[39] Z. Heng, Z. Zeng, Bin Zhang, Y. Luo, J. Luo, Y. Chen, et al., Enhancing mechanical performance of epoxy thermosets via designing a block copolymer to self-organize into “core–shell” nanostructure, RSC Adv. 6 (2016) 77030–77036, https://doi.org/10.1039/C6RA15283J.
[40] S. Ritzenthaler, F. Court, L. David, E. Girard-Reydet, A.L. Leibler, J.P. Pascault, ABC triblock copolymers/epoxy–diamine blends. 1. Keys to achieve nanostructured thermosets, Macromolecules 35 (2002) 6245–6254, https://doi.org/10.1021/ma0121868.
[41] S. Ritzenthaler, F. Court, E. Girard-Reydet, A.L. Leibler, J.P. Pascault, ABC triblock copolymers/epoxy–diamine blends. 2. Parameters controlling the morphologies and properties, Macromolecules 36 (2002) 118–126, https://doi.org/10.1021/ma0211075.
[42] R. Yu, S. Zheng, X. Li, J. Wang, Reaction-induced microphase separation in epoxy thermosets containing block copolymers composed of polystyrene and poly(ε-caprolactone): influence of copolymer architectures on formation of nanophases, Macromolecules 45 (2012) 9155–9168, https://doi.org/10.1021/ma3017212.
[43] M. Martin-Gallego, R. Verdejo, A. Gestos, M.A. Lopez-Manchado, Q. Guo, Morphology and mechanical properties of nanostructured thermoset/block copolymer blends with carbon nanoparticles, Composites A 71 (2015) 136–143, https://doi.org/10.1016/j.compositesa.2015.01.010.
[44] Z. Heng, M. Li, Y. Li, Y. Chen, H. Zou, M. Liang, Spontaneous approach to prepare damping structural integration materials via gradient plasticization mechanism at nanometer scale, Ind. Eng. Chem. Res. 57 (2017) 191–201, https://doi.org/10.1021/acs.iecr.7b03509.
[45] W. Liu, R. Zhou, H.L.S. Goh, S. Huang, X. Lu, From waste to functional additive: toughening epoxy resin with lignin, ACS Appl. Mater. Interfaces 6 (2014) 5810–5817, https://doi.org/10.1021/am500642n.
[46] B. Tang, M. Kong, Q. Yang, Y. Huang, G. Li, Toward simultaneous toughening and reinforcing of trifunctional epoxies by low loading flexible reactive triblock copolymers, RSC Adv. 8 (2018) 17380–17388, https://doi.org/10.1039/C8RA01017J.
[47] J. Wang, Z. Xue, Y. Li, G. Li, Y. Wang, W.-H. Zhong, et al., Synergistically effects of copolymer and core-shell particles for toughening epoxy, Polymer 140 (2018) 39–46, https://doi.org/10.1016/j.polymer.2018.02.031.
[48] Y. Xiang, S. Xu, S. Zheng, Epoxy toughening via formation of polyisoprene nanophases with amphiphilic diblock copolymer, Eur. Polym. J. 98 (2018) 321–329, https://doi.org/10.1016/j.eurpolymj.2017.11.032.
[49] L.-C. Tang, H. Zhang, S. Sprenger, L. Ye, Z. Zhang, Fracture mechanisms of epoxy-based ternary composites filled with rigid-soft particles, Compos. Sci. Technol. 72 (2012) 558–565, https://doi.org/10.1016/j.compscitech.2011.12.015.
[50] Q. Xu, Q. Zhou, K. Shen, D. Jiang, L. Ni, Nanostructured epoxy thermoset templated by an amphiphilic PCL-b-PES-b-PCL triblock copolymer, J. Polym. Sci., Part B: Polym. Phys. 54 (2016) 424–432, https://doi.org/10.1002/polb.23917.
[51] T. Li, S. He, A. Stein, L.F. Francis, F.S. Bates, Synergistic toughening of epoxy modified by graphene and block copolymer micelles, Macromolecules 49 (2016) 9507–9520, https://doi.org/10.1021/acs.macromol.6b01964.
[52] J.D. Liu, Z.J. Thompson, H.-J. Sue, F.S. Bates, M.A. Hillmyer, M. Dettloff, et al., Toughening of epoxies with block copolymer micelles of wormlike morphology, Macromolecules 43 (2010) 7238–7243, https://doi.org/10.1021/ma902471g.
[53] H.S. Tang, T.J.H. Davidock, S.F. Hahn, D.J. Murray, R.C. Cieslinski, N.E. Verghese, et al., Microdeformation behavior in nanotemplated epoxy thermosets: a study with in situ tensile deformation technique in transmission electron microscopy, J. Polym. Sci., Part B: Polym. Phys. 47 (2009) 393–406, https://doi.org/10.1002/polb.21644.
[54] J. Parameswaranpillai, S.P. Ramanan, J.J. George, S. Jose, A.K. Zachariah, S. Siengchin, et al., PEG-ran-PPG modified epoxy thermosets: a simple approach to develop tough shape memory polymers, Ind. Eng. Chem. Res. 57 (2018) 3583–3590, https://doi.org/10.1021/acs.iecr.7b04872.
[55] J. Puig, M. Ceolin, R. Williams, W.F. Schroeder, I.A. Zucchi, Controlling the generation of bilayer and multilayer vesicles in block copolymer/epoxy blends by a slow photopolymerization process, Soft Matter. 13 (2017) 7341–7351, https://doi.org/10.1039/c7sm01660c.